Apaf-1 localization is modulated indirectly by Bcl-2 expression

Antonio Ruiz-Vela*, J.P. Albar, Carlos Martínez-A

Department of Immunology and Oncology, Centro Nacional de Biotecnología/CSIC, Universidad Autónoma de Madrid, Campus de Cantoblanco, E-28049 Madrid, Spain

Received 6 June 2001; accepted 6 June 2001

First published online 29 June 2001

Edited by Veli-Pekka Lehto

Abstract Apoptotic protease activating factor-1 (Apaf-1) is an adaptor molecule essential for caspase-9 activation. Subcellular analysis of Apaf-1 in NIH-3T3 fibroblasts and the immature murine B cell lymphoma WEHI-231 indicates that Apaf-1 is localized in the Golgi apparatus and cytoplasm. Bcl-2 overexpression in WEHI-231 cells disrupts Apaf-1 localization in Golgi, causing a perinuclear Apaf-1 redistribution. Bcl-2 overexpression in NIH-3T3 fibroblasts however does not cause similar Apaf-1 redistribution, suggesting that cell type factors are involved in the redistribution process. The ability of Bcl-2 to modify Apaf-1 subcellular localization is not explained by direct interaction between Apaf-1 and Bcl-2. These data may help to clarify the anti-apoptotic Bcl-2 function.

Key words: B lymphocyte; Apoptosis; Subcellular localization; Bcl-2; Cytochrome *c*; Apaf-1

1. Introduction

The caspases (cysteinyl aspartate-specific proteinases) are essential components in apoptosis [1], as confirmed by the profound defects in apoptosis observed in several caspase knock-out mice. Specifically, cells from caspase-3 or caspase-9 null mutant mice are resistant to apoptosis induced by a variety of signals [2]. Specific cofactor molecules are nonetheless essential for caspase activation in apoptosis [3]. One of these adaptors, Apaf-1 (apoptotic protease activating factor-1), binds caspase-9 via the caspase recruitment domain at its NH_2-terminus, initiating the formation of a supramolecular complex [4,5]. In vitro oligomerization between Apaf-1 and caspase-9 occurs in the presence of cytochrome *c* and dATP, leading to caspase-9 activation and subsequent proteolytic activation of caspase-3 [4]. The apoptotic process triggered by this initiation complex is negatively regulated by the anti-apoptotic Bcl-2 family members. The mechanism used by the anti-apoptotic Bcl-2 family proteins is to block release of proteins normally confined to the mitochondria, including cytochrome *c* [6]. Nonetheless, Bcl-2 is found not only in mitochondria, but is also localized around the nuclear envelope as well as in the endoplasmic reticulum (ER) [7–11], suggesting the existence of additional Bcl-2 functions. In fact, it has been demonstrated that Bcl-2 decreases the free Ca^{2+} concentration within the ER lumen by increasing the Ca^{2+} permeability of the ER membrane [12]. Moreover, Bcl-2 expression increases Ca^{2+} leakage in the ER, thus triggering alterations in the homeostasis of the Golgi apparatus [13].

In the nematode *Caenorhabditis elegans*, one of these additional functions has been characterized for CED-9 (the Bcl-2 homologue); when overexpressed, this molecule sequesters CED-4 (the Apaf-1 homologue) in insoluble subcellular fractions [14]. In mammalian cells, however, no similar function has been identified. Here we report that Bcl-2 regulates the subcellular localization of Apaf-1, illustrated using WEHI-231 and CEM-C7-H.2 lymphocytes as models. We observed that Apaf-1 is localized in Golgi in lymphocytes that do not express Bcl-2, whereas lymphocytes overexpressing Bcl-2 show perinuclear Apaf-1 localization. Taken together, these data indicate a new Bcl-2 function in mammalian cells that appears similar to that observed for CED-9 in *C. elegans*.

2. Materials and methods

2.1. Cell culture

Wild type WEHI-231 and WEHI-231 cells expressing human Bcl-2 (hBcl-2) [15] were cultured in RPMI 1640 medium (BioWhittaker, Walkersville, MD, USA) supplemented with 10% heat-inactivated fetal calf serum (FCS), 2 mM L-glutamine, 100 U/ml penicillin, 100 μg/ml streptomycin, 10 mM HEPES and 50 μM 2-mercaptoethanol (Sigma, St. Louis, MO, USA). NIH-3T3 fibroblasts were cultured in Dulbecco's modified Eagle medium supplemented with 10% FCS and antibiotics as above; both were maintained at 37°C in a humidified 5% CO_2 atmosphere.

2.2. Production and characterization of polyclonal antibodies

Polyclonal anti-Apaf-1 antibody was generated in outbred New Zealand rabbits using a peptide corresponding to the CED-4 domain. The peptide, covering the human APAF-1 sequence 454–469 (QRYHQPHTLSPDQEDC), was synthesized using solid-phase procedure and standard Fmoc chemistry; a C-terminal Cys was included for coupling purposes. The peptide was purified in reverse-phase high performance liquid chromatography (HPLC); purity and composition were confirmed by reverse-phase HPLC and amino acid analysis. For immunization, the peptide was coupled to keyhole limpet hemocyanin (Pierce, Rockford, IL, USA) via the C-terminal Cys. Purified IgG was used for affinity purification. Antibody specificity was confirmed by immunofluorescence in COS cells (Fig. 2), which do no express Apaf-1 protein [16].

2.3. Antibodies and reagents

Antibodies against hBcl-2 (clone 6C8) and mouse Bcl-2 (clone 3F11) were purchased from Pharmingen (San Diego, CA, USA). Anti-protein disulfide isomerase (PDI) antibody (clone 1D3) was purchased from Stressgen (Victoria, BC, Canada). Texas red-conjugated wheat germ agglutinin was purchased from Molecular Probes (Eugene, OR, USA). Anti-β-coat protein (β-COP; clone M3A51) was

*Corresponding author. Fax: (34)-91-372 0493.
E-mail: aruiz@cnb.uam.es

Abbreviations: Apaf-1, apoptotic protease activating factor-1; β-COP, β-coat protein; FCS, fetal calf serum; PDI, protein disulfide isomerase

0014-5793/01/$20.00
PII: S0014-5793(01)02629-1

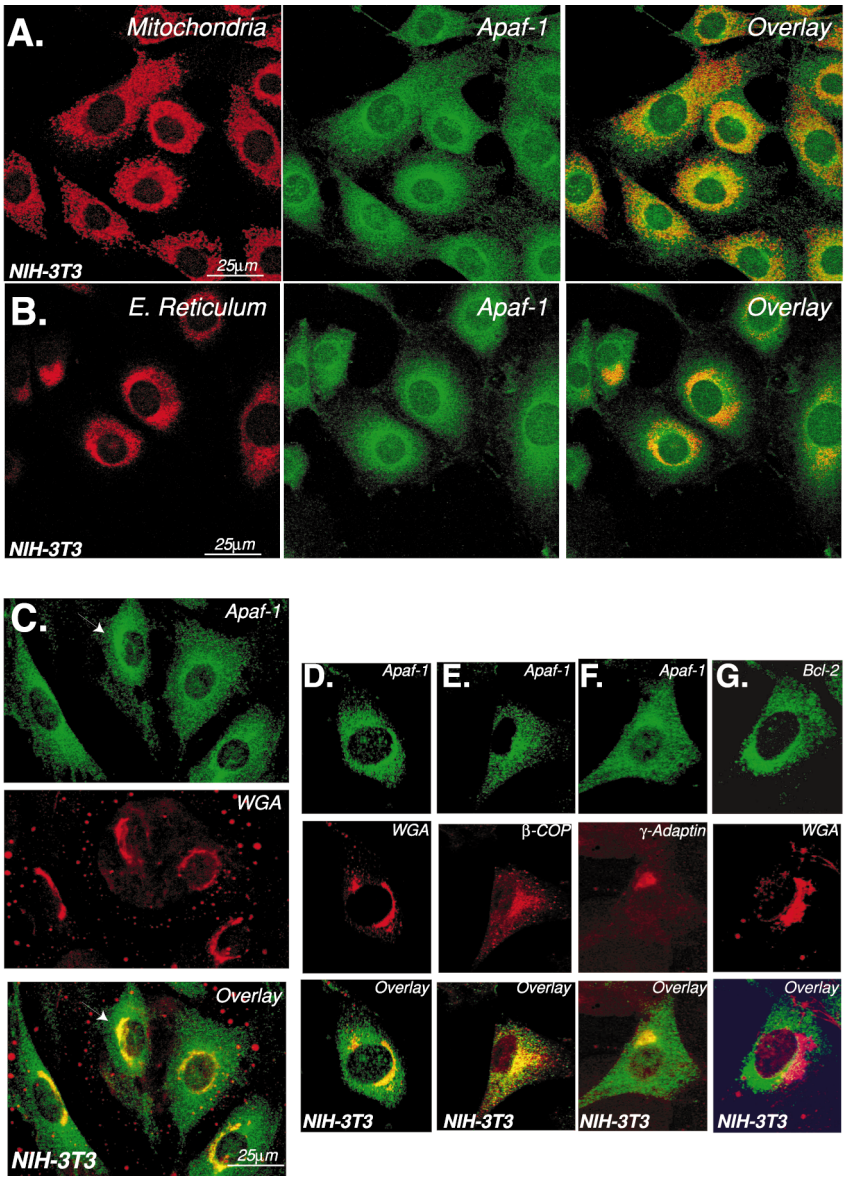
A.
Mitochondria
Apaf-1
Overlay
NIH-3T3
25μm
B.
E. Reticulum
Apaf-1
Overlay
NIH-3T3
25μm
C.
Apaf-1
WGA
Overlay
NIH-3T3
25μm
D.
Apaf-1
WGA
Overlay
NIH-3T3
E.
Apaf-1
β-COP
Overlay
NIH-3T3
F.
Apaf-1
γ-Adaptin
Overlay
NIH-3T3
G.
Bcl-2
WGA
Overlay
NIH-3T3

Fig. 1.

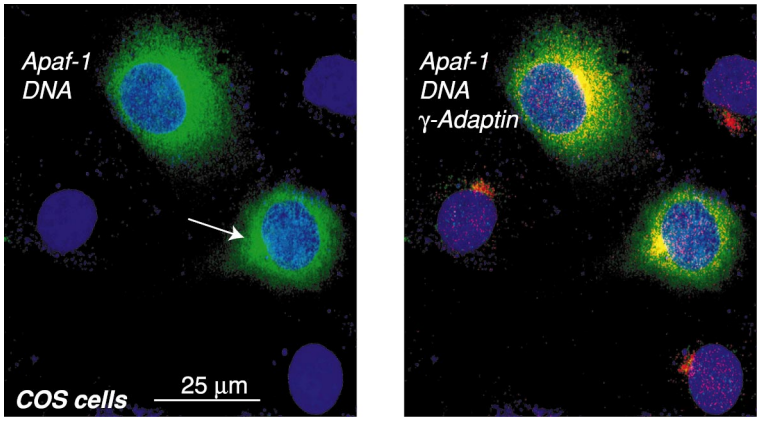
Apaf-1
DNA
COS cells
25 μm
Apaf-1
DNA
γ-Adaptin

Fig. 2.

Fig. 1. Apaf-1 localization in NIH-3T3 fibroblasts. A: Immunofluorescence analysis for Apaf-1 and mitochondria. Cells were treated as described (Section 2). NIH-3T3 fibroblasts were incubated with rabbit anti-Apaf-1 (green fluorescence) and human anti-mitochondrial antibody (red). After incubation, samples were washed, then incubated with Cy2-conjugated anti-rabbit and Cy3-anti-human secondary antibodies. B: Immunofluorescence analysis for Apaf-1 and ER. NIH-3T3 fibroblasts were incubated with rabbit anti-Apaf-1 (green) and anti-PDI antibody (red). After incubation, samples were washed, then incubated with Cy2-conjugated anti-rabbit and Cy3-anti-mouse secondary antibodies. C: Immunofluorescence analysis for Apaf-1 and Golgi. Cells were incubated with anti-Apaf-1 (green) and Texas red-conjugated wheat germ agglutinin (WGA); Cy2-conjugated anti-rabbit antibody was used as second antibody. D: Detail of an NIH-3T3 fibroblast stained for Apaf-1 (green) and Golgi (WGA, red). E: NIH-3T3 fibroblast stained for Apaf-1 (green) and Golgi (β-COP, red); Cy2-anti-rabbit antibody and Cy3-anti-mouse were used as second antibodies. F: NIH-3T3 fibroblast stained for Apaf-1 (green) and Golgi (γ-adaptin, red); Cy2-anti-rabbit antibody and Cy3-anti-mouse were used as second antibodies. G: NIH-3T3 fibroblast stained for Bcl-2 using anti-mouse Bcl-2 (clone 3F11, green) and Golgi (WGA, red); Cy2-anti-rabbit antibody was used as second antibody. The TCS-NT Leica confocal imaging system was used, equipped with a 63×1.4 oil PLAPO objective. Cy2 was analyzed at 488 nm and Cy3/Texas red at 568 nm. Images for each channel were captured separately and assembled into a single file with TCSMERGE software prior to analysis. Confocal images were analyzed using the Leica Vista+ (Beta Release 2) program. Images were processed digitally with Adobe Photoshop (Adobe Systems). The data are representative of the total cell population.
←

from Sigma. Anti-γ-adaptin was purchased from Transduction (Lexington, KY, USA).

2.4. Immunofluorescence and image acquisition

For immunofluorescence, cells were cultured in chamber slides, washed in phosphate-buffered saline (PBS), fixed in 4% paraformaldehyde (15 min, room temperature), pre-incubated in 2% bovine serum albumin (BSA), and incubated for 1 h with primary antibody in PBS containing 0.5% BSA and 0.1% Triton X-100. Cells were washed three times in the same buffer and incubated for 1 h with Cy2- or Cy3-conjugated secondary antibodies (Jackson ImmunoResearch, West Grove, PA, USA). After washing, samples were incubated with TOPRO-3 (Molecular Probes) in PBS for DNA staining. Serial *Z*-sections were obtained using an Ar–Kr laser and a TCS-NT Leica confocal imaging system equipped with a 63×1.4 oil PLAPO objective. Cy2 was analyzed at 488 nm, Cy3 at 568 nm, and TOPRO-3 at 647 nm. Images for each channel were captured separately and assembled into a single file with TCSMERGE software (Leica Microsystems, Heidelberg, Germany) prior to analysis. All confocal images were analyzed using the Leica Vista+ (Beta Release 2) program. Images were processed digitally using Adobe Photoshop (Adobe Systems, Inc.). All the images in the figures represent single sections.

3. Results

CED-9 is the Bcl-2 homologue in the nematode *C. elegans*; when overexpressed, this molecule sequesters CED-4 (the Apaf-1 homologue) in insoluble subcellular fractions [14]. We analyzed Bcl-2 and Apaf-1 localization to study whether Bcl-2 has a similar function in mammalian cells. The cytosolic localization of Apaf-1 has recently been described [16]. To extend the study of Apaf-1 compartmentalization, Apaf-1 subcellular localization was examined by confocal analysis in NIH-3T3 fibroblasts. We analyzed Apaf-1 co-localization with the pyruvate dehydrogenase complex in mitochondria [17], and PDI protein in ER [18], which indicated that Apaf-1 did not co-localize in mitochondria or ER (Fig. 1A,B), confirming previous studies [16]. In contrast, co-localization analysis with distinct Golgi markers showed Apaf-1 in the Golgi apparatus (Fig. 1C–F). This observation was validated by co-localization with (1) wheat germ agglutinin, which binds saccharide moieties in Golgi [19] (Fig. 1C,D), (2) β-COP protein, which is found in Golgi and Golgi-derived (non-clathrin) coated vesicles (Fig. 1E) [20], and (3) γ-adaptin protein in the cytoplasmic face of Golgi and Golgi clathrin-coated vesicles (Fig. 1F) [21]. As a negative control, we analyzed endogenous Bcl-2 in the Golgi apparatus (Fig. 1G). This indicates that, in addition to its cytosolic localization, Apaf-1 is also found in Golgi.

To confirm the immunofluorescence analysis, we overexpressed Apaf-1 in COS cells, which lack the Apaf-1 protein [16]. Apaf-1 overexpression was detected in these cells and clearly expressed in cytoplasm and Golgi in the transfected cells, compared to complete lack of expression in non-transfected COS cells (Fig. 2). These results confirm the antibody specificity, and reinforce the Apaf-1 localization in Golgi in NIH-3T3 cells.

When overexpressed, CED-9 disrupts CED-4 localization in *C. elegans* [14]. To study whether Bcl-2 alters Apaf-1 localization in mammalian cells, we analyzed subcellular Apaf-1 distribution in the immature murine B cell lymphoma WEHI-231 (WEHI-231/wt), as well as in stable WEHI-231 transfectants expressing hBcl-2 (WEHI-231/hBcl-2), which are resistant to apoptosis [15]. In WEHI-231/wt cells, Apaf-1 staining shows a marked structure (Fig. 3A), whereas it surrounds DNA in WEHI-231/hBcl-2 cells, acquiring a perinuclear localization (Fig. 3B). In NIH-3T3 fibroblasts, however, no similar Apaf-1 redistribution is detected when Bcl-2 is overexpressed (Fig. 3C). These results indicate that Bcl-2 strongly disrupts Apaf-1 localization in WEHI-231, but not in NIH-3T3 cells.

To examine the mechanism of Bcl-2-induced Apaf-1 redistribution, we studied Apaf-1 localization in the Golgi apparatus. Apaf-1 clearly localized in Golgi in WEHI-231/wt cells (Fig. 4A), whereas Apaf-1 disappears from Golgi in stable WEHI-231/hBcl-2 transfectants (Fig. 4B). Furthermore, analysis of Apaf-1 and mitochondria indicated that Apaf-1 was not found in mitochondria in either cell type (Fig. 4C,D). Apaf-1 redistribution cannot be explained by interaction between Bcl-2 and Apaf-1, since they did not co-localize in immunofluorescence microscopy (Fig. 4E). The data also indicate that Apaf-1 does not redistribute from Golgi to mitochondria or ER (not shown), where Bcl-2 is localized [7–11], but rather redistributes to the perinuclear space.

←
Fig. 2. Apaf-1 overexpression in COS cells. COS cells were transiently transfected with a clone of Apaf-1 (17) using FuGene 6 (Roche) according to the manufacturer's instructions. At 24 h after transfection, cells were fixed; immunofluorescence analysis was performed (Section 2) to detect Apaf-1 (K-530 antibody, green), Golgi (γ-adaptin, red) and DNA (TOPRO-3, blue). Cy2-anti-rabbit antibody and Cy3-anti-mouse were used as secondary antibodies.

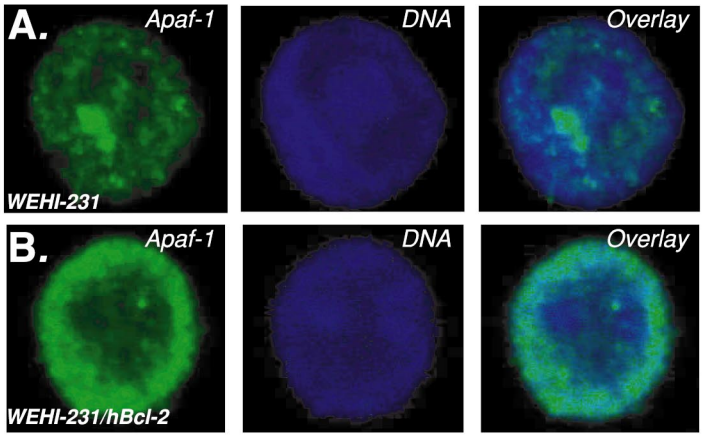
A.
Apaf-1
DNA
Overlay
WEHI-231
B.
Apaf-1
DNA
Overlay
WEHI-231/hBcl-2

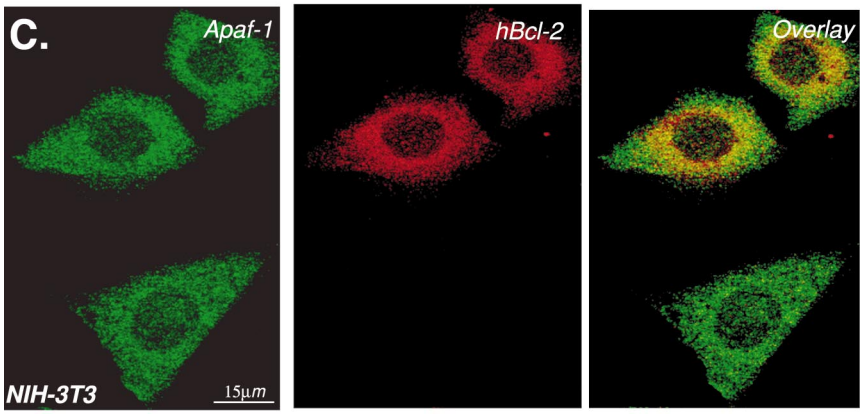
C.
Apaf-1
hBcl-2
Overlay
NIH-3T3
15μm

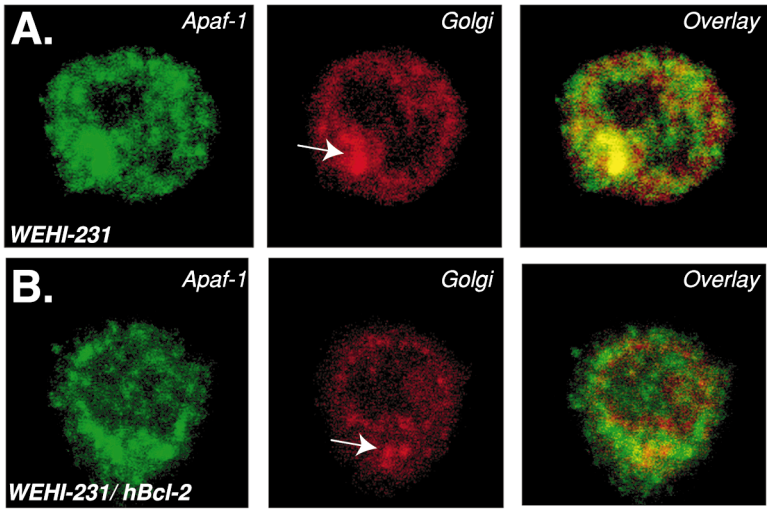
A.
Apaf-1
Golgi
Overlay
WEHI-231
B.
Apaf-1
Golgi
Overlay
WEHI-231/ hBcl-2

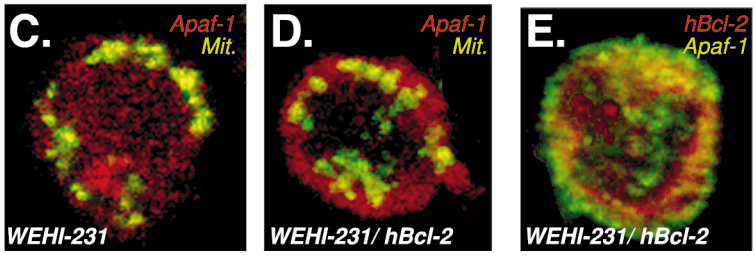
C.
Apaf-1
Mit.
WEHI-231
D.
Apaf-1
Mit.
WEHI-231/ hBcl-2
E.
hBcl-2
Apaf-1
WEHI-231/ hBcl-2

Fig. 3. Apaf-1 localization in WEHI-231/wt and WEHI-231/hBcl-2 cells. A: Immunofluorescence for Apaf-1 and DNA in WEHI-231/wt cells. Immunofluorescence for Apaf-1 (green) using anti-Apaf-1 (K-530) and DNA staining (blue) using TOPRO-3. A detailed image of a cell is shown. B: Immunofluorescence for Apaf-1 and DNA in WEHI-231/hBcl-2 cells. Immunofluorescence for Apaf-1 (green) and DNA staining (blue). A detailed image is shown. C: Bcl-2 overexpression in NIH-3T3 fibroblasts. Cells were transduced with a plasmid containing hBcl-2, produced by cloning a retroviral vector (pCL-Bcl2-Neo) containing hBcl-2 cDNA into the *Eco*RI site of the pCLXSN retroviral plasmid. Retroviral production was carried out by transient transfection of 293T cells. For viral transduction, 10^5 NIH-3T3 fibroblasts were incubated overnight with 5 μg/ml of protamine sulfate (Sigma) in 1 ml of retroviral supernatant or alternatively, in virus-free medium. Infection was performed at 37°C and repeated 24 h later under the same conditions. Transduced NIH-3T3 fibroblasts were treated, washed, fixed, pre-incubated in BSA, and incubated with hamster anti-hBcl-2 (clone 6C8) and anti-Apaf-1 antibodies. After incubation, cells were washed and incubated with Cy3-anti-hamster and Cy2-anti-rabbit secondary antibodies. After washing, optical sections were obtained. The data are representative of the total cell population.
←

4. Discussion

Here we show that Apaf-1 subcellular localization is cell type-dependent and modified by Bcl-2 overexpression. In immunofluorescence microscopy, we show that Bcl-2 induces Apaf-1 redistribution from Golgi apparatus to perinuclear compartments. This effect of Apaf-1 re-localization is not due to interaction between Apaf-1 and Bcl-2. A recent study demonstrates that Apaf-1 does not interact with any Bcl-2 family member [22]; this is supported by our immunofluorescence analysis and yeast two-hybrid system experiments (not shown). This suggests that Bcl-2 triggers Apaf-1 sequestration indirectly, which may explain the cell type specificity of Apaf-1 compartmentalization.

On the other hand, Bcl-2 is found in mitochondria, nuclear envelope and ER [7–11]; in this last compartment, Bcl-2 decreases the free Ca^{2+} concentration within the ER lumen by increasing the Ca^{2+} permeability of the ER membrane [12]. This Bcl-2 function provokes an increase in Ca^{2+} leakage in the ER, triggering alterations in the homeostasis of the Golgi apparatus [13]. Alterations in the distribution of intracellular calcium thus can disturb the mechanism that segregates secretory from resident proteins in ER [23,24]. However, further studies are needed to determine whether the relationship demonstrated here between Apaf-1 and Bcl-2 has a role in in vivo apoptosis.

Acknowledgements: We would like to thank Drs. B.B. Wolf and D.R. Green for reagents and helpful discussions, Dr. G. Nuñez for the hBcl-2 cDNA clone, C. Mark for editorial assistance, and the technical staff of the department who aided with cell culture and material preparations. A.R.V. received a fellowship from the Ministerio de Educación y Cultura. This work was supported by grants from the Spanish Dirección General de Ciencia y Tecnología (DGCyT) and the Ministerio de Educación y Cultura. The Department of Immunology and Oncology was founded and is supported by the Spanish National Research Council (CSIC) and the Pharmacia Corporation.

References

[1] Alnemri, E.S., Livingston, D.J., Nicholson, D.W., Salvesen, G., Thornberry, N.A., Wong, W.W. and Yuan, J. (1996) Cell 87, 171.
[2] Hakem, R., Hakem, A., Duncan, G.S., Henderson, J.T., Woo, M., Soengas, M.S., Elia, A., de la Pompa, J.L., Kagi, D., Khoo, W., Potter, J., Yoshida, R., Kaufman, S.A., Lowe, S.W., Penninger, J.M. and Mak, T.W. (1998) Cell 94, 339–352.
[3] Yoshida, H., Kong, Y.Y., Yoshida, R., Elia, A.J., Hakem, A., Hakem, R., Penninger, J.M. and Mak, T.W. (1998) Cell 94, 739–750.
[4] Li, P., Nijhawan, D., Budihardjo, I., Srinivasula, S.M., Ahmad, M., Alnemri, E.S. and Wang, X. (1997) Cell 91, 479–489.
[5] Zou, H., Henzel, W.J., Liu, X., Lutschg, A. and Wang, X. (1997) Cell 90, 405–413.
[6] Kroemer, G. and Reed, J.C. (2000) Nat. Med. 6, 513–519.
[7] Chen-Levy, Z. and Cleary, M.L. (1990) J. Biol. Chem. 265, 4929–4933.
[8] Chen-Levy, Z., Nourse, J. and Cleary, M.L. (1989) Mol. Cell. Biol. 9, 701–710.
[9] Monaghan, P., Robertson, D., Amos, T.A., Dyer, M.J., Mason, D.Y. and Greaves, M.F. (1992) J. Histochem. Cytochem. 40, 1819–1825.
[10] Allsopp, T.E., Wyatt, S., Paterson, H.F. and Davies, A.M. (1993) Cell 73, 295–307.
[11] Jacobson, M.D., Burne, J.F., King, M.P., Miyashita, T., Reed, J.C. and Raff, M.C. (1993) Nature 361, 365–369.
[12] Foyouzi-Youssefi, R., Arnaudeau, S., Borner, C., Kelley, W.L., Tschopp, J., Lew, D.P., Demaurex, N. and Krause, K.H. (2000) Proc. Natl. Acad. Sci. USA 97, 5723–5728.
[13] Pinton, P., Ferrari, D., Magalhaes, P., Schulze-Osthoff, K., Di Virgilio, F., Pozzan, T. and Rizzuto, R. (2000) J. Cell Biol. 148, 857–862.
[14] Wu, D., Wallen, H.D. and Nuñez, G. (1997) Science 275, 1126–1129.
[15] Brás, A., Ruiz-Vela, A., González de Buitrago, G. and Martínez, A.C. (1999) FASEB J. 13, 931–944.
[16] Hausmann, G., O'Reilly, L.A., van Driel, R., Beaumont, J.G., Strasser, A., Adams, J.M. and Huang, D.C. (2000) J. Cell Biol. 149, 623–634.
[17] Clavería, C., Albar, J.P., Serrano, A., Buesa, J.M., Barbero, J.L. and Martínez-A, C. (1998) EMBO J. 17, 7199–7208.
[18] Huovila, A.P., Eder, A.M. and Fuller, S.D. (1992) J. Cell Biol. 118, 1305–1320.
[19] Virtanen, I., Ekblom, P. and Laurila, P. (1980) J. Cell Biol. 85, 429–434.
[20] Serafini, T., Stenbeck, G., Brecht, A., Lottspeich, F., Orci, L., Rothman, J.E. and Wieland, F.T. (1991) Nature 349, 215–220.
[21] Robinson, M.S. (1990) J. Cell Biol., 2319–2326.
[22] Moriishi, K., Huang, D.C., Cory, S. and Adams, J.M. (1999) Proc. Natl. Acad. Sci. USA 96, 9683–9688.
[23] Sambrook, J.F. (1990) Cell 61, 197–199.
[24] Booth, C. and Koch, G.L. (1989) Cell 59, 729–737.

←
Fig. 4. Apaf-1 localization in Golgi in WEHI-231/wt. A: Immunofluorescence for Apaf-1 and Golgi. Apaf-1 (green) and Golgi stained with Texas red-conjugated wheat germ agglutinin (red). A detail of a WEHI-231/wt cell is shown. B: Immunofluorescence for Apaf-1 and Golgi in WEHI-231/hBcl-2 cells. The arrow indicates the Golgi apparatus. Immunofluorescence for Apaf-1 (red) and mitochondria (green) in WEHI-231/wt (C), for Apaf-1 (red) and mitochondria (green) in WEHI-231/hBcl-2 cells (D), and for Apaf-1 (green) and hBcl-2 (red) in WEHI-231/hBcl-2 cells (E). All samples were treated as described (Section 2). Images are representative of the entire population analyzed.